For example, 'Stage 1' of the original scoring system was defined as 'sparse Lewy bodies or neurites.' On the other hand, 'Grade 1'of our methodology is defined as 'sparse Lewy neurites without Lewy bodies.'

Grade 0 = neither LNs nor LBs detected using anti-phosphorylated α-synuclein antibody.

Grade 1 = sparse phosphorylated α-synuclein immunopositive dots or neurites, or diffuse granular cytoplasmic stain in the neuron, neither LBs nor phosphorylated α-synuclein-immunopositive neuronal intracytoplasmic dense aggregations.

Grade 2 = 1–3 LBs or phosphorylated α-synuclein-immunopositive intracytoplasmic dense aggregations and scattered LNs in a low-power field (×10).

Grade 3 = more than four LBs and scattered LNs in a low-power field (×10).

Grade 4 = numerous LBs and neurites with severe immunoreactivity for phosphorylated α-synuclein in the neuropil or background.

LB staging system of our BBAR (BBAR LB stage)

In order to assess the clinical and neuropathologic alterations of LBD, we applied the following rating system to our BBAR for all autopsy cases (Table 2, Fig. 3). The original BBAR LB staging system was developed in order to track the individual data of our brain bank.[24,25] This rating system requires clinical symptoms, gross and microscopic neuropathologic alterations, and LB scores used in the consensus guidelines for the clinical and pathologic diagnosis of DLB.[27] In this staging system, Parkinson's disease with

Table 2 Lewey body stage of Brain Bank for Aging Research

Stage	Psyn-IR	LB	SN: loss of pigmentation	LB score	Dementia	Parkinsonism	Diagnosis
0	–	–	–				
0.5	+	–	–				
1	+	+	–				Incidental LBD
2	+	+	+	0–10	–†	–†	Subclinical LBD
3	+	+	+	0–10	–	+	PD
4	+	+	+	3–6	+	+	PDDL
	+	+	+	3–6	+	+ or –	DLBL‡
5	+	+	+	7–10	+	+	PDDN
	+	+	+	7–10	+	+ or –	DLBN‡

†Neither dementia nor Parkinsonism associated with Lewy body-related α-synucleinopathy. ‡Differential diagnosis of PDD and DLB was based on the '1-year rule' according to the consensus guidelines (34). DLBL, dementia with Lewy bodies and a Lewy body score corresponding to the limbic form; DLBN, dementia with Lewy bodies and a Lewy body score corresponding to the neocortical form; LB, Lewy body; LBD, Lewy body disease; PD, Parkinson's disease; PDDL, Parkinson's disease with dementia and a Lewy body score corresponding to the limbic form; PDDN, Parkinson's disease with dementia and a Lewy body score corresponding to the neocortical form; Psyn-IR, phosphorylated alpha-synuclein immunoreactivity; SN, substantia nigra.

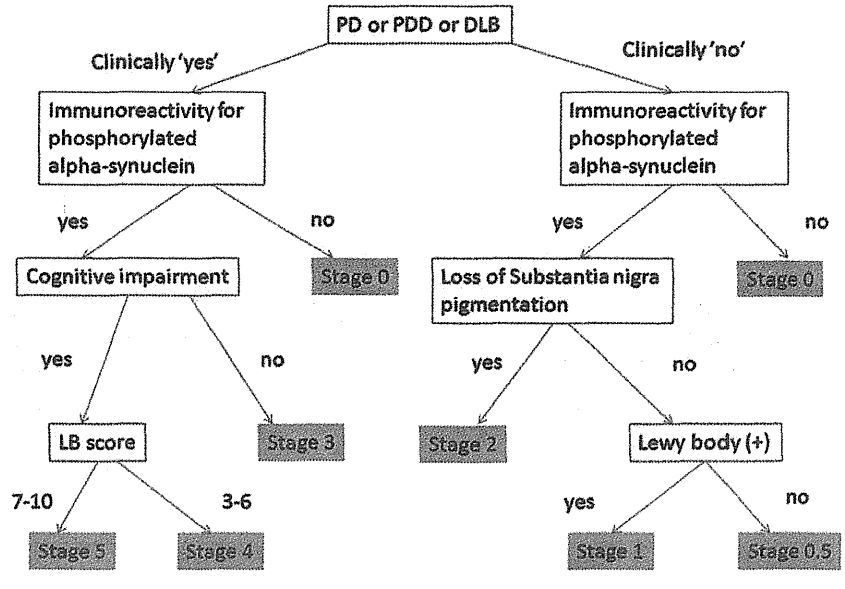

Fig. 3 Flow-chart of the Lewy body staging system of the Brain Bank for Aging Research (BBAR). PD, Parkinson's disease; PDD, Parkinson's disease with dementia; DLB, dementia with Lewy bodies; SN, substantia nigra; LB score, Lewy body score. See Table 2 for detailed description of each stage.

dementia was differentiated from DLB by applying the '12-month (1-year)' rule noted in the Consensus Guidelines (i.e., 'dementia appears more than one year after the onset of Parkinsonism').[27]

Evaluation of senile changes and neuropathologic diagnosis

NFTs were classified according to Braak and Braak's staging system using modified Gallyas-Braak staining[37] and AT8 immunohistochemistry.[38] The staging system for senile plaques (SPs) comprises four stages (0–C). Argyrophilic grains were classified into our four stages (0–III), as reported previously.[23] The neuropathologic diagnosis of Alzheimer disease was based on our previous definition,[39] which proposed a modification of the National Institute on Aging and Reagan Institute criteria.[40,41] The diagnoses of dementia with grains and NFT-predominant forms of dementia were based on the previously described definitions.[42,43]

Statistical analysis

Fisher's exact test was carried out to compare the number of cases having LBAS pathology in the olfactory mucosa.

RESULTS

Clinical information

Of the 105 consecutive autopsy patients, 58 were men and 47 were women. The patient ages at death ranged from 65 to 104 years (82 ± 37, mean ± SD). Twelve patients showed Parkinson's disease-related symptoms according to the clinical criteria in this study. Six out of 105 patients were clinically diagnosed as LBD including Parkinson's disease, Parkinson's disease with dementia and DLB.

Neuropathologic diagnosis

The neuropathologic diagnoses consisted of Alzheimer disease ($n = 15$), dementia with grains ($n = 11$), NFT-predominant form of dementia ($n = 8$), Parkinson's disease ($n = 2$), Parkinson's disease with dementia ($n = 2$), and DLB ($n = 1$), as well as one case each of dentatorubral-pallidoluysian atrophy, neuronal hyaline inclusion body disease, frontotemporal lobar degeneration with transaction response (TAR) DNA-binding protein-43 kDa-immunoreactive inclusions, and progressive multifocal leukoencephalopathy. Patients with combined pathologies, included Alzheimer's disease plus DLB ($n = 2$), dementia with grains plus NFT-predominant form of dementia ($n = 3$), and one patient each of diffuse NFTs with calcification (DNTC)[44] plus DLB and dementia with grains plus Alzheimer's disease. The remaining patients did not fulfil the clinical and/or pathological criteria for neurodegenerative diseases.

Eight out of 105 patients (8/105 = 7.6%) were clinically and neuropathologically diagnosed as having LBD, including Parkinson's disease (2 patients), Parkinson's disease with dementia (2 patients) and DLB (4 patients).

Incidence, distribution and extent of LBAS

BBAR staging

Based on clinical and neuropathologic analyses, the BBAR LB stages were as follows: stage 0 = 66 cases, stage 0.5 = 6 cases, stage 1 = 21 cases, stage 2 = 4 cases, stage 3 = 2 cases, stage 4 = 3 cases and stage 5 = 3 cases. All of the stage 5 cases had DLB, with an LB score corresponding to the value for the neocortical form (DLBN).

LBAS in CNS and peripheral nervous system

We identified 39 (37.1%) out of the 105 individuals with α-synuclein immunopositive LBAS in the CNS or peripheral nervous system (Table 3). Therefore, we focused on these 39 cases in the present study. Here, LBAS was identified by using α-synuclein immunohistochemistry. In LBAS, LBs were confirmed with HE stains and α-synuclein immunohistochemistry. Out of the 39 cases, 33 showed LBAS in the olfactory bulb, 15 in the enteric nerve plexus, 23 in the sympathetic ganglia, and 16 in the pericardial nerve fibers of the left ventricle (Tables 3 and 4).

Olfactory mucosa

The olfactory epithelium is a pseudostratified columnar epithelium lying deep within the recess of the superior nasal cavity; it is composed of a mixture of multipotential stem cells (basal cells), supporting cells and olfactory receptor neurons (Fig. 2). Mature neurons are reported to give rise to fine and unmyelinated axons that ascend through the cribriform plate to synapse at glomeruli in the olfactory bulb.[20,45]

LBAS were found in the olfactory mucosa of seven (17.9%) out of 39 cases (Tables 3 and 4). These seven also had LBAS in the olfactory bulb. LBAS was present in the lamina propria mucosa of the seven cases (Fig. 4a–c). In addition, one case showed LBAS in a bundle of axons in the cribriform plate (Fig. 4d). None of the cases showed LBAS in the olfactory epithelial paraneuron. We summarized the demographic results of these seven individuals with LBAS in the olfactory mucosa in Table 5. Neither phosphorylated tau-positive deposits nor amyloid β immunopositive deposits were detected in the olfactory mucosa.

Table 3 The distribution of α-synuclein deposits in various anatomical regions of 39 cases with Lewy body disease

Age at death/gender	Parietal lobe	Frontal lobe	Temporal lobe	Cingulate gyrus	Entorhinal cortex	Amygdala	Olfactory bulb	Nucleus basalis of Meynert	Substantia nigra	Locus coeruleus	Dorsal motor nucleus of the vagus	Spinal Cord	Gastrointestinal system	Olfactory Mucosa	Sympathetic ganglion	Adrenal gland	Pericardial nerve	Skin	BBAR LB stage	NFT stage	SP stage
104/F																			5	4	C
70/F																			5	4	C
86/F																			5	6	C
84/M																			4	2	A
79/F																			4	2	A
80/F																			4	2	A
81/M																			3	2	A
88/M																			3	3	A
79/M																			2	1	A
68/F																			2	2	B
79/F																			2	6	C
77/F																			2	6	C
78/M																			1	2	A
75/M																			1	2	A
89/F																			1	3	C
93/F																			1	4	C
86/M																			1	4	C
81/M																			1	2	A
90/F																			1	2	A
86/M																			1	2	A
97/F																			1	2	A
78/M																			1	1	A
92/M																			1	3	C
94/M																			1	4	A
85/M																			1	3	A
81/F																			1	5	C
96/F																			1	2	0
87/F																			1	3	A
101/F																			1	4	A
69/F																			1	4	0
83/F																			1	3	A
72/M																			1	1	A
77/M																			1	2	A
83/M																			0.5	4	C
71/M																			0.5	2	A
89/M																			0.5	2	A
85/F																			0.5	3	A
85/F																			0.5	2	A
96/F																			0.5	3	A

Grade 0 = blank, grade 1 = light grey, grade 2 = light blue, grade 3 = blue, grade4 = navy blue. The number in each cell indicates a score based on the semiquantitative scoring system of Lewy-related pathology. 0 = neither Lewy neurites nor bodies detected by using anti-phosphorylated α-synuclein antibody. 1 = sparse phosphorylated α-synuclein immunopositive dots or neurites, neither Lewy bodies nor phosphorylated α-synuclein immunopositive intracytoplasmic aggregations. 2 = one to three Lewy bodies or phosphorylated α-synuclein immunopositive intracytoplasmic aggregations in a low-power field (×10). 3 = more than four Lewy bodies and scattered Lewy neurites in a low-power field (×10). 4 = numerous LBs and neurites with severe immunoreactivity for phosphorylated α-synuclein in the neuropil or background. Individuals of BBAR LB stages 3–5, with clinical Parkinsonism and neuropathologically numerous LBASs in the CNS, showed high incidence (75%, 6/8 individuals) of LBASs in the olfactory mucosa. In contrast, individuals of BBAR LB stages 1–3 without Parkinsonism showed extremely low incidence of Lewy body-related α-synucleinopathy (LBAS) (3%, 1/31) in the olfactory mucosa. LBAS was found in the olfactory mucosa mostly in advanced BBAR LB stages 3–5. BBAR LB Brain Bank for Aging Research Lewy body staging, NFT stage, Braak's stages for neurofibrillary tangles; SP stage, Braak's stages for senile plaques.

Table 4 Regional frequency of Lewy body-related α-synucleinopathy (LBAS) in various anatomical regions

The BBAR LB stage	Olfactory epithelium	Olfactory mucosa	Olfactory bulb	Spinal cord	GI tract	Sympathetic ganglia	Adrenal gland	Pericardial nerve	Skin
0.5	0/6	0/6	2/6	0/6	0/6	2/6	0/6	1/6	0/6
1	0/21	1/21	19/21	7/21	6/27	10/21	1/21	6/21	1/21
2	0/4	0/4	4/4	3/4	1/4	3/4	0/4	2/4	0/4
3	0/2	1/2	2/2	2/2	2/2	2/2	2/2	1/2	2/2
4	0/3	3/3	3/3	3/3	3/3	3/3	3/3	3/3	2/3
5	0/3	2/3	3/3	3/3	3/3	3/3	1/3	3/3	0/3
All	**0/39**	**7/39**	**33/39**	**18/39**	**15/39**	**23/39**	**7/39**	**16/39**	**5/39**

BBAR LB Brain Bank for Aging Research Lewy body staging.

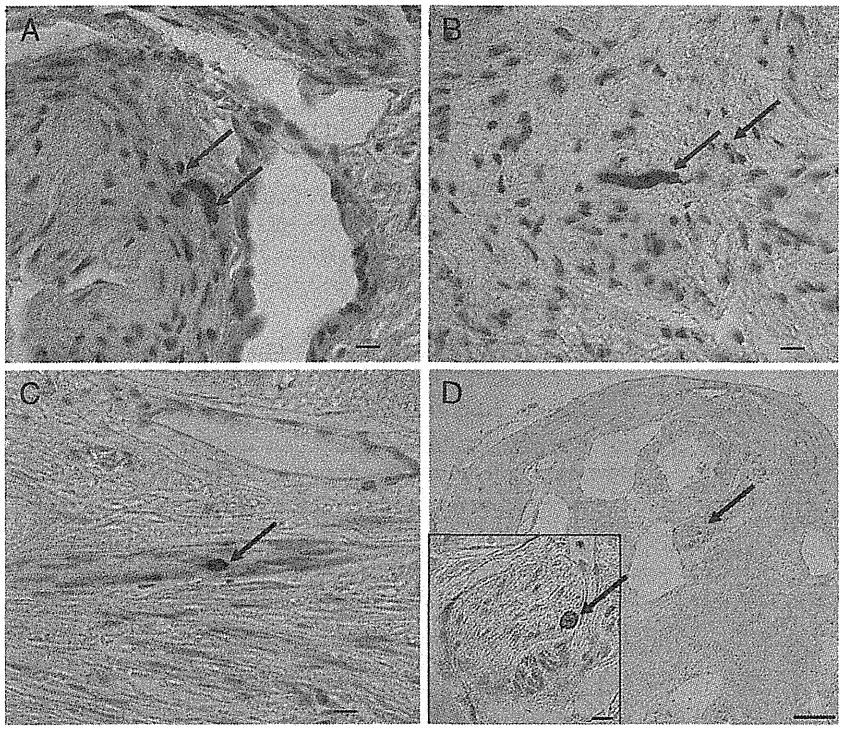

Fig. 4 Photomicrographs show α-synuclein immunopositive deposits (arrows indicate Lewy neurites) in the axonal bundle of the lamina propria (a–c) and cribriform plate (d). The inset in figure (d) shows a higher magnification image of α-synuclein immunopositive deposits in the axonal bundle of the cribriform plate. Immunohistochemistry using monoclonal antibody against phosphorylated α-synuclein (pSyn#64). Photomicrographs (a, b, c and d) were obtained from cases 4, 5, 7 and 3, respectively, in Table 5. (a–c), scale bar = 10 μm; (d) scale bar = 100 μm (inset, 10 μm).

Correlations between α-synuclein immunopositive LBs or LNs in the olfactory mucosa and CNS

Alpha-synuclein immunopositive LBs or LNs in the olfactory mucosa were detected in seven cases, including three with DLB, three with Parkinson's disease or Parkinson's disease with dementia, and one with incidental LBD (Tables 3–5). LBAS in the olfactory mucosa was compared with those in other locations of the CNS (Table 3). Individuals of BBAR LB stages 3–5, clinical and neuropathological diagnosis of LBD, showed a high incidence (75%, 6/8 individuals) of α-synuclein immunopositive LBAS in the olfactory mucosa (Table 6, Fig. 5). Six individuals with Parkinson's disease also showed a high incidence of α-synuclein accumulation (66%, 4/6 individuals) in the olfactory mucosa. In contrast, individuals of BBAR LB stages 0.5–2 (here we classified them into asymptomatic group) showed a low incidence of LBAS (3%, 1/31) in the olfactory mucosa.

Olfactory bulb

There is neural connectivity among olfactory receptor neurons and nuclei in the olfactory bulbs.[45] Hence, we analyzed the frequency of LBAS in the glomeruli, tufted cells, mitral cells and granular cells between LBAS-positive and LBAS-negative groups in the olfactory epithelium.

In individuals of BBAR LB stages 3–5 (symptomatic stage), LBAS was frequently observed in the glomeruli (8/8 cases, 100%), granular cells (8/8, 100%) and tufted cells (7/8, 87.5%). In contrast, there were low numbers of cases with LBAS in the mitral cells (2/8, 25%). Asymptomatic stage cases of LBD, corresponding to BBAR stage 0.5–2,

Table 5 Clinical and neuropathological demography of seven individuals with Lewy body-related α-synucleinopathy (LBAS) identified in the olfactory mucosa

No.	Age at death	Clinically diagnosed as LBD	Cause of death	Neuropathologic diagnosis	BBAR LB stage	LBAS in the olfactory mucosa			NFT stage	SP stage
						Olfactory epithelium	Lamina propria mucosa	Cribriform plate		
1	104/F	None	CHF, MI, Dementia	DLBN, AD	5	0	1	0	1	C
2	70/F	DLB	DLB, pneumonia	DLBN, AD	5	0	1	0	1	C
3	84/M	DLB	Prostate carcinoma, DLB	DLBL	4	0	1	1	2	A
4	79/F	PDD	PDD	PDDN	4	0	1	0	2	A
5	80/F	PD	Pneumonia, PD	PDDL	4	0	1	0	2	A
6	88/M	PD	Pneurmonia, PD	PD	3	0	1	0	2	A
7	86/M	None	Pneumonia	AD,Incidental LBD	1	0	1	0	1	C

AD, Alzheimer's disease; BBAR LB stage, Lewy body staging system of the Brain Bank for Aging Research; CHF, congestive heart failure; DLB, dementia with Lewy bodies; DLBL, dementia with Lewy bodies and a Lewy body score corresponding to the limbic form; DLBN, dementia with Lewy bodies and a Lewy body score corresponding to the neocortical form; F, female; LB, Lewy body; LBD, Lewy body disease; M, male; MI, acute myocardial infarction; NFT stage, Braak's stages for neurofibrillary tangles; PD, Parkinson's disease; PDDL, Parkinson's disease with dementia and a Lewy body score corresponding to the limbic form; PDDN, Parkinson's disease with dementia and a Lewy body score corresponding to the neocortical form; SP stage, Braak's stages for senile plaques.

Table 6 Incidence of LBAS in the olfactory mucosa in cases with symptomatic LBD (BBAR stage 3–5)

Clinical and neuropathologic diagnosis of LBD	LBAS in OM		Total
	Present	Absent	
Symptomatic (BBAR 3–5)	6*	2	8
Asymptomatic (BBAR 0.5–2)	1	30	31

*$P < 0.05$. BBAR, Brain Bank for Aging Research; LBAS; Lewy body-related alpha-synucleinopathy; LBD, Lewey body disease; OM; olfactory mucosa.

showed high incidence of LBAS in the glomeruli (23/31, 74.1%) and granular cells (22/31, 70.9%) of the olfactory bulb (Fig. 5).

DISCUSSION

Our study provides two novel observations.

1 LBAS in the olfactory mucosa was frequently observed (6/8 cases, 75%) in the symptomatic patients with LBD, but was a rare condition (1/31 cases, 3.2%) in asymptomatic LBD patients.
2 LBAS was seen in the glomeruli and granular cells in the olfactory bulbs of most symptomatic and asymptomatic cases with LBD.

It has been widely accepted that LB pathology does not develop simultaneously in all anatomical regions of the central and peripheral nervous systems. Hawkes *et al.* proposed that neurotropic pathogens may enter the brain via two routes: (i) a nasal route, with anterograde progression into the temporal lobe; and (ii) a gastric route secondary to the swallowing of nasal secretions in saliva (a dual hit hypothesis).[46] The former route may be associated with the early accumulation of α-synuclein in the human olfactory bulb and cause olfactory dysfunction in sporadic Parkinson's disease. In the present study, there was rare observation of LBAS in the olfactory mucosa in the asymptomatic cases of LBD. Further analysis is important to clarify the possibility of propagation of α-synuclein in the nervous systems.

In the present study, LBAS was frequently observed in the olfactory mucosa (6/8 cases, 75%) in the individuals with clinical LBD. In contrast, LBAS in the olfactory mucosa was a rare observation in asymptomatic patients. It is also important that all seven cases with LBAS in the olfactory mucosa had LBAS in the cerebral cortex and brainstem. Our results have similarities with a previous report concerning Alzheimer's disease.[20] Detection of LBAS in the olfactory mucosa could be hindered by two problems: technical difficulty in obtaining enough nerve fibers and rapid turnover of olfactory receptor neurons.[47,48] In fact, a recent study reported that a biopsy study revealed no α-synuclein immunopositive deposits in the olfactory

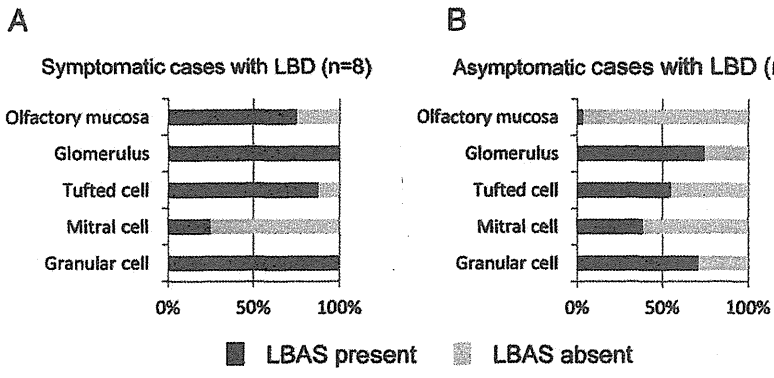

Fig. 5 Frequencies of cases having Lewy-related α-synucleinopathy (LBAS) pathology in the olfactory mucosa and each anatomical region of the olfactory bulb. (a) Cases with symptomatic dementia with Lewy bodies (LBD) ($n = 8$, Brain Bank for Aging Research [BBAR] stages 3–5). Most of the cases show LBAS pathology in the olfactory mucosa (6/8, 75%), glomeruli (8/8, 100%), tufted cells (6/7, 85.7%) and granular cells (8/8, 100%). The number of cases with LBAS in the mitral cells is low (2/6, 33.3%). (b) Cases with asymptomatic LBD ($n = 25$, BBAR stages 0.5–2). Most of the cases show LBAS pathology in the glomeruli (23/31, 74.1%), tufted cells (17/31, 54.8%) and granular cells (22/31, 70.9%). The number of cases with LBAS in the mitral cells (12/31, 38.7%) is low. LBAS pathology of the olfactory mucosa is present in only one case (1/31, 3.2%).

mucosa of patients of Parkinson's disease.[21] Our previous study indicated a high incidence of α-synuclein immunopositive LBs or neurites in aging human olfactory bulbs, and suggested that they extend from the periphery (the second olfactory structure) to the anterior olfactory nucleus (the tertiary olfactory structure).[11] The present study, using 6 μm-thick paraffin embedded sections, revealed that LBAS was most frequently observed in the glomeruli which were composed of axon terminals of olfactory epithelial cells and dendrites of mitral and tufted cells[45] as well as in the glomerular cells which were most numerous in the periphery of the olfactory bulb (Fig. 5). We consider that high incidence of LBAS in glomeruli may represent affected terminal axons of olfactory epithelial neurons. In contrast to our result, a previous study, employing 50 μm-thick floating sections, reported high frequency of LBAS in mitral cells and the internal plexiform layer in individuals with Parkinson's disease but no LBAS in age-matched controls.[49] Further studies are necessary to identify the most vulnerable subset in the periphery of the olfactory bulb.

In conclusion, presence of LBAS in the olfactory mucosa and olfactory glomeruli further supports the importance of olfactory system as an entry zone of LBD. Future studies of LB pathology involving the olfactory system are indicated to understand the pathomechanism of α-synuclein accumulation in individuals with LBD.

ACKNOWLEDGMENTS

This study was supported in part by a Grant-in-Aid for Scientific Research (Kakenhi B) (20390248) (SM), The Specified Disease Treatment Research Program (SM), Research on Measures for Intractable Diseases (MT) (H23-nanchi-ippan-062, H24-nanchi-ippan-063, Nanchi-ippan-013), and the Comprehensive Brain Science Network (SM, MT). We gratefully acknowledge Naoo Aikyo, Fumio Hasegawa, Mieko Harada, Yuki Kimura, Nobuko Naoi and Sachiko Imai for technical help. We thank Dr. T. Iwatsubo (Department of Neuropathology, University of Tokyo, Tokyo, Japan) for the kind gifts of antibodies and Dr. K. Suzuki (Department of Neuropathology, Tokyo Metropolitan Geriatric Hospital and Institute of Gerontology) for useful discussions and comments.

Portions of this study were presented at the 86th annual meeting of the American Association of Neuropathologists, Philadelphia, in 2010.

REFERENCES

1. Baba M, Nakajo S, Tu PH *et al.* Aggregation of alpha-synuclein in Lewy bodies of sporadic Parkinson's disease and dementia with Lewy bodies. *Am J Pathol* 1998; **152**: 879–884.
2. Spillantini MG, Crowther RA, Jakes R, Hasegawa M, Goedert M. alpha-Synuclein in filamentous inclusions of Lewy bodies from Parkinson's disease and dementia with Lewy bodies. *Proc Natl Acad Sci U S A* 1998; **95**: 6469–6473.
3. Goedert M, Spillantini MG, Davies SW. Filamentous nerve cell inclusions in neurodegenerative diseases. *Curr Opin Neurobiol* 1998; **8**: 619–632.
4. Ogunnyi A, Akang EE, Gureje O *et al.* Dementia with Lewy bodies in a Nigerian: a case report. *Int Psychogeriatr* 2002; **14**: 211–218.
5. Takao M, Ghetti B, Yoshida H *et al.* Early-onset dementia with Lewy bodies. *Brain Pathol* 2004; **14**: 137–147.
6. Braak H, Ghebremedhin E, Rub U, Bratzke H, Del Tredici K. Stages in the development of Parkinson's disease-related pathology. *Cell Tissue Res* 2004; **318**: 121–134.
7. Braak H, Sastre M, Bohl JR, de Vos RA, Del Tredici K. Parkinson's disease: lesions in dorsal horn layer I,

involvement of parasympathetic and sympathetic pre- and postganglionic neurons. *Acta Neuropathol* 2007; **113**: 421–429.
8. Braak H, Braak E. Pathoanatomy of Parkinson's disease. *J Neurol* 2000; **247** (Suppl 2): II3–110.
9. Braak H, Del Tredici K, Rub U, de Vos RA, Jansen Steur EN, Braak E. Staging of brain pathology related to sporadic Parkinson's disease. *Neurobiol Aging* 2003; **24**: 197–211.
10. Del Tredici K, Rub U, De Vos RA, Bohl JR, Braak H. Where does Parkinson disease pathology begin in the brain? *J Neuropathol Exp Neurol* 2002; **61**: 413–426.
11. Sengoku R, Saito Y, Ikemura M *et al.* Incidence and extent of Lewy body-related alpha-synucleinopathy in aging human olfactory bulb. *J Neuropathol Exp Neurol* 2008; **67**: 1072–1083.
12. Ponsen MM, Stoffers D, Booij J, van Eck-Smit BL, Wolters ECh, Berendse HW. Idiopathic hyposmia as a preclinical sign of Parkinson's disease. *Ann Neurol* 2004; **56**: 173–181.
13. Haehner A, Boesveldt S, Berendse HW *et al.* Prevalence of smell loss in Parkinson's disease – a multicenter study. *Parkinsonism Relat Disord* 2009; **15**: 490–494.
14. Daniel SE, Hawkes CH. Preliminary diagnosis of Parkinson's disease by olfactory bulb pathology. *Lancet* 1992; **340** (8812): 186.
15. Pearce RK, Hawkes CH, Daniel SE. The anterior olfactory nucleus in Parkinson's disease. *Mov Disord* 1995; **10**: 283–287.
16. Beach TG, White CL 3rd, Hladik CL *et al.* Olfactory bulb alpha-synucleinopathy has high specificity and sensitivity for Lewy body disorders. *Acta Neuropathol* 2009; **117**: 169–174.
17. Parkkinen L, Silveira-Moriyama L, Holton JL, Lees AJ, Revesz T. Can olfacotry bulb biopsy be justified for the diagnosis of Parkinson's disease? Comments on 'olfactory bulb α-synucleinopathy has specificity and sensitivity for Lewy body disorders'. *Acta Neuropathol* 2009; **117** (2): 213–214.
18. Jellinger KA. Olfactory bulb α-synucleinopathy has specificity and sensitivity for Lewy body disorders. *Acta Neuropathol* 2009; **117** (2): 215–216.
19. Duda JE, Shah U, Arnold SE, Lee VM, Trojanowski JQ. The expression of alpha-, beta-, and gamma-synucleins in olfactory mucosa from patients with and without neurodegenerative diseases. *Exp Neurol* 1999; **160**: 515–522.
20. Arnold SE, Lee EB, Moberg PJ *et al.* Olfactory epithelium amyloid-beta and paired helical filament-tau pathology in Alzheimer disease. *Ann Neurol* 2010; **67**: 462–469.
21. Witt M, Bormann K, Gudziol V *et al.* Biopsies of olfactory epithelium in patients with Parkinson's disease. *Mov Disord* 2009; **24**: 906–914.
22. Fumimura Y, Ikemura M, Saito Y *et al.* Analysis of the adrenal gland is useful for evaluating pathology of the peripheral autonomic nervous system in Lewy body disease. *J Neuropathol Exp Neurol* 2007; **66**: 354–362.
23. Saito Y, Ruberu NN, Sawabe M *et al.* Staging of argyrophilic grains: an age-associated tauopathy. *J Neuropathol Exp Neurol* 2004; **63**: 911–918.
24. Saito Y, Ruberu NN, Sawabe M *et al.* Lewy body-related alpha-synucleinopathy in aging. *J Neuropathol Exp Neurol* 2004; **63**: 742–749.
25. Saito Y, Kawashima A, Ruberu NN *et al.* Accumulation of phosphorylated alpha-synuclein in aging human brain. *J Neuropathol Exp Neurol* 2003; **62**: 644–654.
26. Ikemura M, Saito Y, Sengoku R *et al.* Lewy body pathology involves cutaneous nerves. *J Neuropathol Exp Neurol* 2008; **67**: 945–953.
27. McKeith IG, Galasko D, Kosaka K *et al.* Consensus guidelines for the clinical and pathologic diagnosis of dementia with Lewy bodies (DLB): report of the consortium on DLB international workshop. *Neurology* 1996; **47**: 1113–1124.
28. Folstein MF, Folstein SE, McHugh PR. 'Mini-mental state'. A practical method for grading the cognitive state of patients for the clinician. *J Psychiatr Res* 1975; **12**: 189–198.
29. Hasegawa K Inoue K, Moriya K. An investigation of dementia rating scale for the elderly. *Seishin Igaku* 1974; **16**: 965–969.
30. Hosokawa T, Yamada Y, Isagoda A, Nakamura R. Psychometric equivalence of the Hasegawa Dementia Scale-Revised with the Mini-Mental State Examination in stroke patients. *Percept Mot Skills* 1994; **79**: 664–666.
31. Lawton MP, Brody EM. Assessment of older people: self-maintaining and instrumental activities of daily living. *Gerontologist* 1969; **9**: 179–186.
32. Morris JC. The Clinical Dementia Rating (CDR): current version and scoring rules. *Neurology* 1993; **43**: 2412–2414.
33. McKhann G, Drachman D, Folstein M, Katzman R, Price D, Stadlan EM. Clinical diagnosis of Alzheimer's disease: report of the NINCDS-ADRDA Work Group under the auspices of Department of Health and Human Services Task Force on Alzheimer's Disease. *Neurology* 1984; **34**: 939–944.
34. McKeith IG, Dickson DW, Lowe J *et al.* Diagnosis and management of dementia with Lewy bodies: third report of the DLB Consortium. *Neurology* 2005; **65**: 1863–1872.

35. Gallyas F. Silver staining of Alzheimer's neurofibrillary changes by means of physical development. *Acta Morphol Acad Sci Hung* 1971; **19**: 1–8.
36. Fujiwara H, Hasegawa M, Dohmae N *et al.* alpha-Synuclein is phosphorylated in synucleinopathy lesions. *Nat Cell Biol* 2002; **4**: 160–164.
37. Braak H, Braak E. Neuropathological stageing of Alzheimer-related changes. *Acta Neuropathol* 1991; **82**: 239–259.
38. Braak H, Alafuzoff I, Arzberger T, Kretzschmar H, Del Tredici K. Staging of Alzheimer disease-associated neurofibrillary pathology using paraffin sections and immunocytochemistry. *Acta Neuropathol* 2006; **112**: 389–404.
39. Murayama S, Saito Y. Neuropathological diagnostic criteria for Alzheimer's disease. *Neuropathology* 2004; **24**: 254–260.
40. Consensus recommendations for the postmortem diagnosis of Alzheimer's disease. The National Institute on Aging, and Reagan Institute Working Group on Diagnostic Criteria for the Neuropathological Assessment of Alzheimer's Disease. *Neurobiol Aging* 1997; **18**: S1–S2.
41. Hyman BT, Trojanowski JQ. Consensus recommendations for the postmortem diagnosis of Alzheimer disease from the National Institute on Aging and the Reagan Institute Working Group on diagnostic criteria for the neuropathological assessment of Alzheimer disease. *J Neuropathol Exp Neurol* 1997; **56**: 1095–1097.
42. Jellinger KA. Dementia with grains (argyrophilic grain disease). *Brain Pathol* 1998; **8**: 377–386.
43. Jellinger KA, Bancher C. Senile dementia with tangles (tangle predominant form of senile dementia). *Brain Pathol* 1998; **8**: 367–376.
44. Kosaka K. Diffuse neurofibrillary tangles with calcification: a new presenile dementia. *J Neurol Neurosurg Psychiatry* 1994; **57**: 594–596.
45. Hawkes CH, Doty RL. *The Neurology of Olfaction.* Cambridge, UK: Cambridge University Press, 2009; 16–21.
46. Hawkes CH, Del Tredici K, Braak H. Parkinson's disease: a dual-hit hypothesis. *Neuropathol Appl Neurobiol* 2007; **33**: 599–614.
47. Graziadei PP, Okano M. Neuronal degeneration and regeneration in the olfactory epithelium of pigeon following transection of the first cranial nerve. *Acta Anat (Basel)* 1979; **104**: 220–236.
48. Graziadei PP, Monti Graziadei AG. Regeneration in the olfactory system of vertebrates. *Am J Otolaryngol* 1983; **4**: 228–233.
49. Ubeda-Bañon I, Saiz-Sanchez D, de la Rosa-Prieto C, Argandoña-Palacios L, Garcia-Muñozguren S, Martinez-Marcos A. alpha-Synucleinopathy in the human olfactory system in Parkinson's disease: involvement of calcium-binding protein- and substance P-positive cells. *Acta Neuropathol* 2010; **119**: 723–735.

BMJ open accessible medical research

Multicentre multiobserver study of diffusion-weighted and fluid-attenuated inversion recovery MRI for the diagnosis of sporadic Creutzfeldt–Jakob disease: a reliability and agreement study

Koji Fujita,[1] Masafumi Harada,[2] Makoto Sasaki,[3] Tatsuhiko Yuasa,[4] Kenji Sakai,[5] Tsuyoshi Hamaguchi,[5] Nobuo Sanjo,[6] Yusei Shiga,[7] Katsuya Satoh,[8] Ryuichiro Atarashi,[8] Susumu Shirabe,[9] Ken Nagata,[10] Tetsuya Maeda,[10] Shigeo Murayama,[11] Yuishin Izumi,[1] Ryuji Kaji,[1] Masahito Yamada,[5] Hidehiro Mizusawa[6]

To cite: Fujita K, Harada M, Sasaki M, *et al*. Multicentre, multiobserver study of diffusion-weighted and fluid-attenuated inversion recovery MRI for the diagnosis of sporadic Creutzfeldt–Jakob disease: a reliability and agreement study. *BMJ Open* 2012;**2**: e000649. doi:10.1136/bmjopen-2011-000649

► Prepublication history for this paper is available online. To view this file please visit the journal online (http://bmjopen.bmj.com).

Received 21 November 2011
Accepted 20 December 2011

For numbered affiliations see end of article.

Correspondence to
Dr Masafumi Harada;
masafumi@clin.med.tokushima-u.ac.jp

ABSTRACT

Objectives: To assess the utility of the display standardisation of diffusion-weighted MRI (DWI) and to compare the effectiveness of DWI and fluid-attenuated inversion recovery (FLAIR) MRI for the diagnosis of sporadic Creutzfeldt–Jakob disease (sCJD).

Design: A reliability and agreement study.

Setting: Thirteen MRI observers comprising eight neurologists and five radiologists at two universities in Japan.

Participants: Data of 1.5-Tesla DWI and FLAIR were obtained from 29 patients with sCJD and 13 controls.

Outcome measures: Standardisation of DWI display was performed utilising b0 imaging. The observers participated in standardised DWI, variable DWI (the display adjustment was observer dependent) and FLAIR sessions. The observers independently assessed each MRI for CJD-related lesions, that is, hyperintensity in the cerebral cortex or striatum, using a continuous rating scale. Performance was evaluated by the area under the receiver operating characteristics curve (AUC).

Results: The mean AUC values were 0.84 (95% CI 0.81 to 0.87) for standardised DWI, 0.85 (95% CI 0.82 to 0.88) for variable DWI and 0.68 (95% CI 0.63 to 0.72) for FLAIR, demonstrating the superiority of DWI ($p<0.05$). There was a trend for higher intraclass correlations of standardised DWI (0.74, 95% CI 0.66 to 0.83) and variable DWI (0.72, 95% CI 0.62 to 0.81) than that of FLAIR (0.63, 95% CI 0.53 to 0.74), although the differences were not statistically significant.

Conclusions: Standardised DWI is as reliable as variable DWI, and the two DWI displays are superior to FLAIR for the diagnosis of sCJD. The authors propose that hyperintensity in the cerebral cortex or striatum on 1.5-Tesla DWI but not FLAIR can be a reliable diagnostic marker for sCJD.

ARTICLE SUMMARY

Article focus

- Evaluation of the reliability of diffusion-weighted imaging (DWI) display standardisation for the diagnosis of sporadic Creutzfeldt–Jakob disease (sCJD).
- Comparison between DWI and fluid-attenuated inversion recovery (FLAIR) for the diagnosis of sCJD.

Key messages

- Standardised DWI display is as reliable as observer-dependent DWI display.
- DWI is superior to FLAIR for the diagnosis of sCJD.
- Hyperintensity in the cerebral cortex or striatum on 1.5-Tesla DWI but not FLAIR can be a reliable diagnostic marker for sCJD.

Strengths and limitations of this study

- Strength of this study is the large number of physicians who participated in the observer performance study.
- This study was limited by the retrospective nature that may lead to a selection bias.

INTRODUCTION

Reliable detection of Creutzfeldt–Jakob disease (CJD) is imperative for infection control and treatment. MRI is useful for the early diagnosis of CJD,[1 2] whereas the utility of EEG and conventional cerebrospinal fluid (CSF) tests have been limited.[3] Diffusion-weighted imaging (DWI) and fluid-attenuated inversion recovery (FLAIR) are key techniques for the diagnosis of sporadic CJD (sCJD) with high sensitivity and specificity when assessed by expert neurologists or

neuroradiologists.[1 4 5] However, the utility of MRI for general neurologists or radiologists who are not familiar with diagnosing CJD remains elusive. Moreover, standardisation of MRI methodologies, which would be essential for the reproducible assessment of MRI findings of CJD cases, has not been achieved in previous studies.[1 4 5] DWI display conditions may particularly vary among institutions or operators,[6] which can give rise to inaccurate assessment of CJD-related lesions, specifically subtle abnormalities in the cerebral cortex. Meanwhile, although DWI seems superior to FLAIR for the detection of CJD lesions,[5] direct comparison of the two sequences is yet to be performed.

To address these issues, we investigated the utility of a newly proposed standardisation method of DWI display[6 7] and compared the effectiveness of DWI and FLAIR for the diagnosis of sCJD, particularly for differentiating between abnormal and normal signals by neurologists and radiologists who are not necessarily CJD experts. We conducted a multicentre, multiobserver case–control study and evaluated observer performance with receiver operating characteristics (ROC) analysis.

METHODS

Subjects

Patients diagnosed as having sCJD by the CJD Surveillance Committee of Japan[8] from October 2005 to September 2010 were eligible to participate in this study. The accuracy of the diagnosis was defined as follows: definite, that is, pathologically verified cases; probable, that is, cases with neuropsychiatric manifestations compatible with sCJD and periodic sharp wave complexes on EEG without pathological examinations and possible, that is, cases with the same findings as probable sCJD but no periodic sharp wave complexes on EEG.[8 9] WHO criteria[10] were not applied because the assay of CSF 14-3-3 protein, which is required by WHO criteria, was standardised only since April 2009 in Japan.[11] The prion protein gene (*PRNP*) was analysed in the open reading frame after extracting DNA from patients' blood.[12 13] For neuropathological examinations, brain sections were stained with routine techniques, and immunohistochemistry was performed using the mouse monoclonal antibody 3F4 (Senetek, MD Heights, Missouri, USA).[12] For PrP^{Sc} typing, frozen brain tissues were homogenised and analysed by western blot for proteinase K-resistant PrP using the 3F4 antibody.[14] Assays for CSF γ-isoform of 14-3-3 protein,[11] total τ protein (cut-off value, 1300 pg/ml)[15] and real-time quaking-induced conversion (RT-QUIC)[16] were performed in patients whose CSF samples were available. The following patients were eligible as disease controls: patients who were suspected to have prion disease by primary physicians but were denied to have prion disease by the Committee or those who were diagnosed as having other neurological disorders at Tokushima University Hospital and whose brain MRI showed no abnormal intensity in the cerebral cortex or striatum. We requested physicians who had referred patients to the Committee to provide initial MRI data of eligible patients.

This study was approved by the Medical Ethics Committee of Kanazawa University and the Ethics Committees of the Tokushima University Hospital and Tokyo Medical and Dental University. Written informed consent was obtained from all patients or their families.

Magnetic resonance imaging

DWI, b0 and FLAIR images were converted to the Digital Imaging and Communication in Medicine format. When the Digital Imaging and Communication in Medicine data contained patient information, it was excluded by one of the investigators (MH) before the observer performance study. All MRI studies were performed on 1.5-Tesla scanners at each hospital. Quadrature detection head coils or multichannel head coils were used. DWI was performed using the single-shot spin-echo echo planar imaging technique with the following parameters: repetition time, 4000–8000 ms; echo time, 70–100 ms; b value, 1000 s/mm^2; slice thickness, 5 mm; matrix size, 128×80 to 128×128; field of view, 220–230 mm and 16–20 contiguous axial sections parallel to a line through the anterior and posterior commissures were obtained from each patient. The scanning parameters of FLAIR were as follows: repetition time, 8000–10 000 ms; inversion time, 2000–2500 ms; effective echo time, 105–120 ms; matrix size, 256×192 to 320×224; field of view, 210–220 mm; slice thickness, 5–6 mm with 1–1.5 mm interslice gaps and 19–20 slices per patient.

Display methods

Two display methods were used for DWI: standardised and variable. In the standardised display, the window width and level settings were constant for all evaluations and could not be changed. Details of the standardised display have been reported elsewhere.[6] In brief, the window width and level were as follows: window width = SI_{b0} and window level = $SI_{b0}/2$, where SI_{b0} represents the signal intensity in the normal-appearing subcortical region on b0 imaging.[6] One radiologist (MH) manually measured SI_{b0} within a circular region of interest. The calculated window width and level were applied to all images. In the variable display mode, regarded as the most reliable for assessment of DWI, each observer was able to change the window width and level settings on the monitor according to preference. FLAIR was assessed with the variable display method because no standardised methods are currently available for FLAIR display.

Observer performance study

Eight neurologists (6–27 years of experience; mean, 12 years; board certified, six) and five radiologists (5–25 years of experience; mean, 12.8 years; board certified, four; neuroradiologist, one) participated in the observer performance study at The University of Tokushima Graduate School (persons, six; neurologists, three) and Tokyo Medical and Dental University

(persons, seven; neurologists, five including NS and YS). Before the test, the observers were informed that the purpose of the study was to evaluate their performance in detecting MRI lesions compatible with CJD, that is, hyperintensity in the cerebral cortex or striatum, regardless of signal changes in other regions including the thalamus. Three sessions were conducted: standardised DWI, variable DWI and FLAIR. To reduce the effect of learning, the interval between reading sessions was 1 week or longer. The order of the three sessions was randomised among the observers. Using computer randomisation, images of patients with and without sCJD were intermixed. All cases were presented in the same randomised order to the observers in each session. Each observer independently viewed all slices of each MRI study on the same type of monitors (Let'snote, Panasonic, Osaka, Japan) using INTAGE Realia Professional (Cubernet, Tokyo, Japan) run on Windows XP (Microsoft). The observers were allowed to adjust the window width and level only in variable DWI and FLAIR sessions but not in the standardised DWI session. Observers were blinded to any clinical information including age, sex and diagnosis.

Each observer used a continuous rating scale of a line-marking method to rate his or her confidence level on the paper format independently. At the left end of the line, a confidence level that lesions compatible with CJD were definitely absent was indicated, whereas at the right end, a confidence level that lesions were definitely present was indicated. Intermediate levels of confidence were indicated by the different positions on the line between the two ends. The distance between the left end and the marked point was converted to a confidence level that could range from 0 to 100, as described elsewhere.[17]

Statistical analyses

Observer performance was evaluated using ROC analysis with SPSS V.19 (IBM). The ROC curves for each observer indicated the ratio of the true-positive fraction to the false-positive fraction at each confidence level. The area under the ROC curve (AUC) was used to compare observer performance for accurately detecting CJD lesions. Intraclass correlations were calculated in the neurologist group, the radiologist group and for all observers by two-way random consistency measures using the SPSS software. In all the analyses, p values of <0.05 were considered statistically significant.

RESULTS

Patients and controls

MRI data from 85 patients were provided. Of these, 42 subjects from 15 hospitals (including authors' institutions) were eligible for this study after excluding cases that were diagnosed as having non-sporadic CJD or lacked the required MRI sequences. This study cohort included 29 patients with sCJD (men, 11; mean age, 71 years; duration before MRI, 4.4±6.1 months), three patients who were suspected of CJD but eventually diagnosed as negative by the Committee and 10 patients diagnosed as having other neurological disorders. Of the 29 sCJD patients, four had definite, 24 had probable and one had possible CJD. Twenty-six cases underwent *PRNP* analysis, 24 were homozygous for methionine at codon 129 and two were heterozygous with methionine and valine at codon 129. Of the four definite cases, PrP^{Sc} was type 1 in two cases, type 1+2 in one case and type 2 in one case. Eleven of 15 CSF samples from probable sCJD cases were positive for PrP^{Sc} by RT-QUIC (table 1).

Diagnoses for three prion-denied patients were immune-mediated encephalopathy, juvenile Alzheimer's disease and frontotemporal dementia. Other neurological controls were diagnosed with Alzheimer's disease, Parkinson's disease, spinocerebellar degeneration, vascular dementia, old cerebral infarction, benign paroxysmal positional vertigo, dizziness, temporal arteritis, cervical spondylosis and diabetic neuropathy.

Diagnostic performance

We investigated the diagnostic performance of standardised DWI, variable DWI and FLAIR images assessed by eight neurologists and five radiologists using ROC analysis. Mean AUC values obtained from the three sessions were compared within the neurologist group, the radiologist group and all observers (figure 1, table 2). The AUC values for standardised and variable DWI were not different within each professional group or for the total observer group. On the other hand, AUC values for FLAIR were significantly lower than DWI displayed by either method ($p<0.05$). Representative MRI scans are shown in figure 2.

Rating agreement

To measure the extent to which the observers agreed when rating the MRI findings, intraclass correlations were calculated. The intraclass correlations of the standardised DWI (0.74, 95% CI 0.66 to 0.83) and variable DWI (0.72. 95% CI 0.62 to 0.81) tend to be higher than that of FLAIR (0.63, 95% CI 0.53 to 0.74), specifically in the neurologist group, although the differences were not significant (figure 3).

DISCUSSION

We demonstrated that standardised DWI was as useful as variable DWI and that both DWI displays are superior to FLAIR for the diagnosis of sCJD when assessed by multiobservers with various specialty backgrounds.

Our standardisation method of DWI display was originally proposed as an easy-to-use way to decide the window width and level for DWI even in emergency settings.[6] Indeed, this method was demonstrated as useful for detecting acute ischaemic lesions on DWI.[7] Results of the present study show that the standardisation method is also reliable for diagnosis of sCJD, in which DWI is one of the key sequences. We suggest some advantages of standardised DWI over variable DWI, although there was no statistical difference between the two methods. First, standardised DWI can be helpful for

Table 1 Clinical profiles of patients with sporadic Creutzfeldt–Jakob disease

No	Age/sex	Diagnosis	Codon129/PrP^{Sc}	14-3-3/total τ	RT-QUIC	Pre-MRI duration (months)
1	69/M	Definite	MM/1	+/+	+	–2*
2	77/F	Definite	MM/1	+/+	+	19
3	75/F	Definite	ND/1+2	+/+	+	3
4	65/M	Definite	MM/2	–/–	–	12
5	69/M	Probable	MM	ND	–	0.5
6	72/F	Probable	MM	ND	ND	0.5
7	77/F	Probable	MM	–/–	+	0.5
8	72/M	Probable	MM	ND	ND	1
9	63/M	Probable	MM	+/+	+	1.5
10	88/F	Probable	MM	ND	ND	1.5
11	75/M	Probable	MV	ND	ND	1.5
12	56/M	Probable	MM	+/+	+	2
13	67/M	Probable	MM	+/+	–	2
14	70/M	Probable	MM	+/+	+	2
15	70/F	Probable	MM	+/+	+	2
16	74/F	Probable	MM	+/+	–	2
17	84/F	Probable	MM	+/–	+	2
18	85/F	Probable	MM	–/+	+	2
19	49/F	Probable	ND	+/+	+	2
20	74/F	Probable	MV	+/+	+	2.5
21	54/F	Probable	ND	ND	ND	2.5
22	61/M	Probable	MM	ND	ND	3
23	72/F	Probable	MM	+/–	–	3
24	81/F	Probable	MM	–/–	+	3
25	70/M	Probable	MM	+/+	+	6
26	83/F	Probable	MM	+/+	ND	9
27	67/F	Probable	MM	+/+	–	15
28	84/F	Probable	MM	+/+	–	26
29	57/F	Possible	MM	ND	ND	4

*MRI was obtained 2 months before the symptom onset.[2]
MM, homozygous for methionine; MV, heterozygous with methionine and valine; ND, not done; RT-QUIC, real-time quaking-induced conversion.

physicians who can refer only to hardcopies but not softcopies. Second, even for doctors who can readily refer to softcopies and thus variable DWI, the standardisation method can simplify assessment procedure without any disadvantages. Third, the standardisation can facilitate direct comparison of DWI findings from different CJD patients.

DWI and FLAIR have been reported as useful markers for the diagnosis of CJD. Of these, DWI has been assumed to be the most sensitive, although without direct evidence.[1 5 18] Hyperintensity in the cerebral cortices, the striatum or both indicates the diagnosis of CJD. The striatum hyperintensity is anterior dominant at early stages of the disease.[19] MRI lesion profiles reportedly differ among molecular subtypes of sCJD,[20 21] which was not reproduced in a recent study.[5] Zerr *et al*[4] proposed that high-signal abnormalities in caudate nucleus and putamen or at least two cortical regions (temporal, parietal or occipital lobes) either in DWI or FLAIR together with typical clinical signs can be diagnostic for probable sCJD. Based partly upon their report, 'high signal in caudate/putamen on MRI brain scan' has

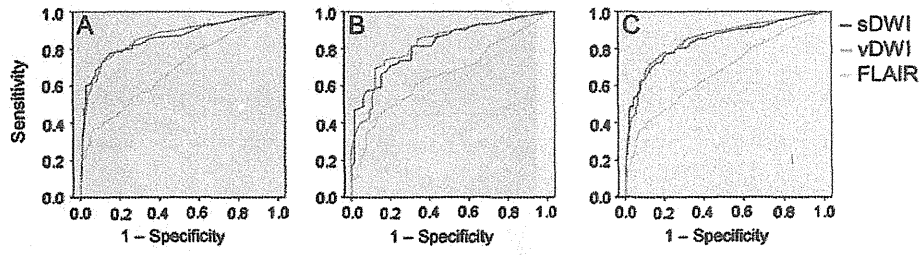

Figure 1 Receiver operating characteristic curves for each display in diagnosis of sporadic Creutzfeldt–Jakob disease. (A) Neurologists, (B) radiologists and (C) all observers. The true rate (sensitivity) is plotted as a function of the false-positive rate (1 – specificity). DWI, diffusion-weighted imaging; FLAIR, fluid-attenuated inversion recovery; sDWI, standardised DWI; vDWI, variable DWI.

Table 2 Areas under the receiver operating characteristic curves

	Neurologists	Radiologists	All observers
sDWI	0.86 (0.82 to 0.90)	0.82 (0.77 to 0.88)	0.84 (0.81 to 0.87)
vDWI	0.86 (0.82 to 0.90)	0.83 (0.77 to 0.89)	0.85 (0.82 to 0.88)
FLAIR	0.69 (0.63 to 0.75)	0.66 (0.58 to 0.73)	0.68 (0.63 to 0.72)

Means (95% CIs) are indicated.
DWI, diffusion-weighted imaging; FLAIR, fluid-attenuated inversion recovery; sDWI, standardised DWI; vDWI, variable DWI.

been used as one of the laboratory findings in the diagnostic criteria for probable sCJD in the European CJD Surveillance System (EUROCJD) since January 2010.[22] However, their criteria did not distinguish DWI and FLAIR, thereby maintaining ambiguity about the diagnostic values of MRI in situations where DWI is not available. Our data indicate that FLAIR without DWI is unreliable for the diagnosis of sCJD. On the other hand, high signals in the cerebral cortex have not been regarded as diagnostic in the EUROCJD criteria, probably because cortical abnormalities are less reliable on conventional MRI. Our results suggest that, using standardised or variable DWI but not FLAIR, cortical signals can also be used as a diagnostic marker.

Meanwhile, Young *et al*[23] reported that the sensitivity and the specificity of DWI and FLAIR for the diagnosis of CJD are 91% and 95%, respectively. More recently, Vitali *et al*[5] reported that hyperintensity greater on DWI than FLAIR is diagnostic for sCJD, whereas hyperintensity greater on FLAIR than DWI is characteristic for non-prion rapidly progressive dementia. Furthermore, reduction of apparent diffusion coefficient in subcortical (striatum) hyperintensity regions on DWI is supportive for sCJD.[5 24 25] These findings can be greatly helpful for differentiating sCJD from other rapidly progressive dementia. However, assessment of FLAIR lesions tends to vary among physicians, particularly among neurologists, as shown by the present study, and standardised methods for FLAIR or apparent diffusion coefficient map have not been established until date. Therefore, clinical criteria which require DWI but not necessarily FLAIR or apparent diffusion coefficient will be more readily applicable.

As many as 13 neurologists and radiologists from different institutions participated in the observer performance study, although the sample size of patients was relatively small. Notably, the observers had various specialty backgrounds such as stroke neurologists, neurophysiologists, experts in dementia or prion disease and general and neuroradiologists. This variety simulates practical situations in which the diagnosis of suspected CJD cases may be made by physicians who do not necessarily specialise in prion disease.

This study has some limitations. First, we did not evaluate patterns of cortical involvement suggestive of sCJD[4 5] because we had to address whether DWI or FLAIR is suitable for detecting cortical lesions in the first place. Second, we did not assess the difference among sCJD subtypes[21] because majority of our cases had a typical phenotype and were homozygous for methionine; thus, they were compatible with MM1 sCJD. Until date, MM2 thalamic-type sCJD remains a diagnostic challenge in MRI-based assessment; thalamic hypoperfusion or hypometabolism on SPECT or PET can be useful.[26] Third, majority of the control patients were not those who were suspected to have CJD. However, the

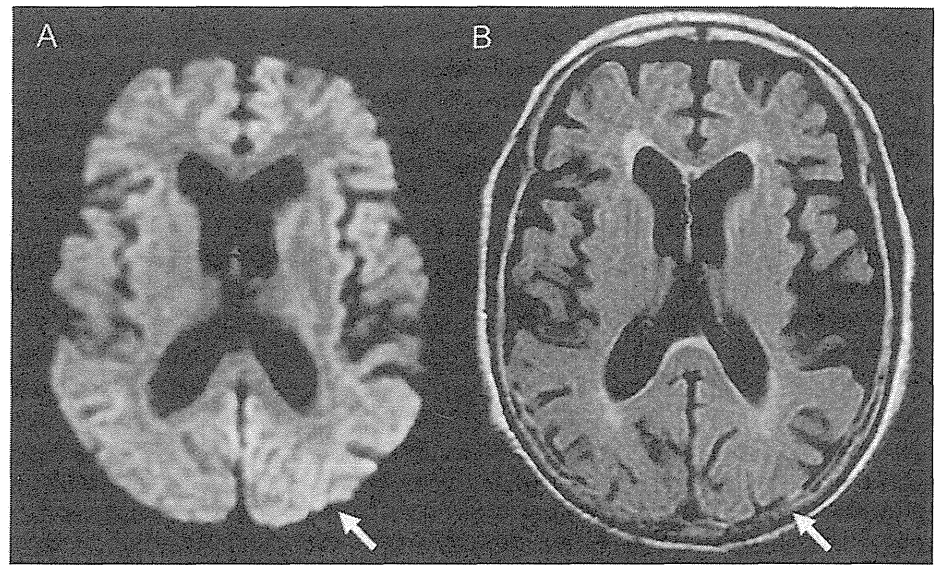

Figure 2 Representative MRI of a sporadic Creutzfeldt–Jakob disease patient (case 17). Abnormal hyperintensity in the cerebral cortex is evident on standardised diffusion-weighted imaging (A, arrow) but obscure on fluid-attenuated inversion recovery (B, arrow).

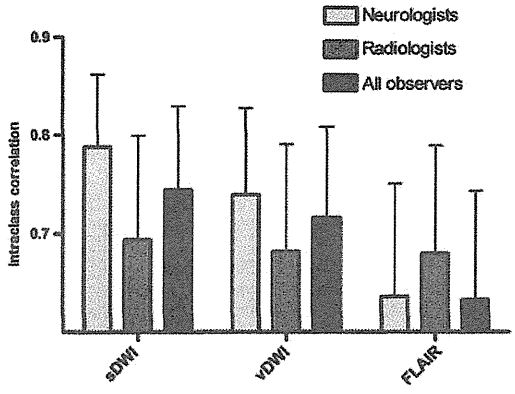

Figure 3 Intraclass correlations for each display. Error bars represent upper limits of 95% CIs. DWI, diffusion-weighted imaging; FLAIR, fluid-attenuated inversion recovery; sDWI, standardised DWI; vDWI, variable DWI.

principle aim of the present study was to establish a display method, which reliably distinguishes potentially CJD-associated signals from normal signals. Thus, our results provide a practical foundation for utilising DWI as a general diagnostic marker of sCJD when combined with previous findings.[1 4 5]

Although neuropathological confirmation of the diagnosis of sCJD was obtained in few cases, we performed RT-QUIC, a newly established CSF PrP^{Sc} amplification assay which achieved >80% sensitivity and 100% specificity for CJD.[16] Overall, 15 of 29 cases (51.7%) were pathologically proven or confirmed by RT-QUIC to have CJD. There were no significant differences in MRI findings between sCJD patients with and without positive results of CSF 14-3-3 protein, total τ protein or RT-QUIC. It will be important to further evaluate accurate diagnostic ability (sensitivity and specificity) of DWI in a prospective cohort of suspected CJD patients, that is, consecutive patients registered to the CJD surveillance who will also undergo CSF confirmation tests or neuropathological analyses.

In conclusion, we suggest that hyperintensity in the cerebral cortex or striatum assessed on the standardised or variable DWI scanned with 1.5-Tesla machines can be a reliable first-line on-site diagnostic marker for sCJD.

Author affiliations
[1]Department of Clinical Neuroscience, Institute of Health Biosciences, The University of Tokushima Graduate School, Tokushima, Japan
[2]Department of Radiology, Institute of Health Biosciences, The University of Tokushima Graduate School, Tokushima, Japan
[3]Advanced Medical Science Center, Iwate Medical University, Morioka, Japan
[4]Department of Neurology, Kamagaya-Chiba Medical Center for Intractable Neurological Disease, Kamagaya General Hospital, Kamagaya, Japan
[5]Department of Neurology and Neurobiology of Aging, Kanazawa University Graduate School of Medical Science, Kanazawa, Japan
[6]Department of Neurology and Neurological Science, Graduate School, Tokyo Medical and Dental University, Tokyo, Japan
[7]Department of Neurology, Aoba Neurosurgical Clinic, Sendai, Japan
[8]Department of Molecular Microbiology and Immunology, Nagasaki University Graduate School of Biomedical Sciences, Nagasaki, Japan
[9]Center for Health and Community Medicine, Nagasaki University, Nagasaki, Japan
[10]Department of Neurology, Research Institute for Brain and Blood Vessels, Akita, Japan
[11]Department of Neuropathology (Brain Bank for Aging Research), Tokyo Metropolitan Institute of Gerontology, Tokyo, Japan

Acknowledgements We thank Tetsuyuki Kitamoto (Tohoku University Graduate School of Medicine) for *PRNP* analysis, western blotting of PrP and neuropathological investigations; Yuka Terasawa, Yoshimitsu Shimatani, Ai Miyashiro (Department of Clinical Neuroscience, The University of Tokushima Graduate School), Hideki Otsuka, Naomi Morita, Yoichi Otomi (Department of Radiology, The University of Tokushima Graduate School), Satoru Ishibashi, Takumi Hori, Akira Machida (Department of Neurology and Neurological Science, Tokyo Medical and Dental University), Isamu Ohashi and Takashi Katayama (Department of Radiology, Tokyo Medical and Dental University) for participation in the observer performance study. We also thank Joe Senda (Nagoya University), Yuko Nemoto (Chiba Medical Center), Akio Kawakami (Kaetsu Hospital), Isao Sasaki (Mizunomiyako Memorial Hospital), Shigeyuki Kojima (Matsudo Municipal Hospital), Motohiro Yukitake (Saga University), Hiroyuki Murai (Iizuka Hospital), Hideki Mizuno (Kohnan Hospital), Akira Arai (Aomori Prefectural Central Hospital), Masamitsu Yaguchi (Shinoda General Hospital), Takanori Oikawa (South Miyagi Medical Center) and all other collaborative physicians for providing MRI data of the patients. We thank the members of the CJD Surveillance Committee of Japan for their support of this work.

Funding This study was supported by Grants-in-Aid from the Research Committee of Surveillance and Infection Control of Prion Disease and from the Research Committee of Prion Disease and Slow Virus Infection, the Ministry of Health, Labour and Welfare of Japan.

Competing interests None.

Patient consent Obtained.

Ethics approval This study was approved by the Medical Ethics Committee of Kanazawa University and the Ethics Committees of the Tokushima University Hospital and Tokyo Medical and Dental University.

Contributors KF, MH, MS, TY, KSak, TH, NS, YS, KSat, SS, MY and HM: design/conceptualisation of the study. MH, KSak, TH, NS, YS, KSat, RA, KN, TM, SM and YI: acquisition of data. KF, MH, MS, RA, RK, MY and HM: analysis/interpretation of the data. MH: statistical analyses. KF, MH, MS, TY, KSak, TH, NS, YS, KSat, RA, SS, KN, TM, SM, YI, RK, MY and HM: drafting/revising the manuscript. All authors contributed to final approval of the version to be published.

Provenance and peer review Not commissioned; externally peer reviewed.

Data sharing statement There are no additional data available.

REFERENCES

1. Shiga Y, Miyazawa K, Sato S, *et al.* Diffusion-weighted MRI abnormalities as an early diagnostic marker for Creutzfeldt–Jakob disease. *Neurology* 2004;63:443–9.
2. Satoh K, Nakaoke R, Nishiura Y, *et al.* Early detection of sporadic CJD by diffusion-weighted MRI before the onset of symptoms. *J Neurol Neurosurg Psychiatry* 2011;82:942–3.
3. Chitravas N, Jung RS, Kofskey DM, *et al.* Treatable neurological disorders misdiagnosed as Creutzfeldt–Jakob disease. *Ann Neurol* 2011;70:437–44.
4. Zerr I, Kallenberg K, Summers DM, *et al.* Updated clinical diagnostic criteria for sporadic Creutzfeldt–Jakob disease. *Brain* 2009;132:2659–68.
5. Vitali P, Maccagnano E, Caverzasi E, *et al.* Diffusion-weighted MRI hyperintensity patterns differentiate CJD from other rapid dementias. *Neurology* 2011;76:1711–19.
6. Sasaki M, Ida M, Yamada K, *et al.* Standardizing display conditions of diffusion-weighted images by using concurrent b0 images: a multivendor multi-institutional study. *Magn Reson Med Sci* 2007;6:133–7.
7. Hirai T, Sasaki M, Meada M, *et al*; Acute Stroke Imaging Standardization Group-Japan (ASIST-Japan). Diffusion-weighted imaging in ischemic stroke: effect of display method on observers' diagnostic performance. *Acad Radiol* 2009;16:305–12.
8. Nozaki I, Hamaguchi T, Sanjo N, *et al.* Prospective 10-year surveillance of human prion diseases in Japan. *Brain* 2010;133:3043–57.
9. Masters CL, Harris JO, Gajdusek DC, *et al.* Creutzfeldt–Jakob disease: patterns of worldwide occurrence and the significance of familial and sporadic clustering. *Ann Neurol* 1979;5:177–88.

10. WHO. Global surveillance, diagnosis and therapy of human transmissible spongiform encephalopathies: report of a WHO consultation. *World Health Organization: Emerging and Other Communicable Diseases, Surveillance and Control.* Geneva: WHO, 1998.
11. Satoh K, Tobiume M, Matsui Y, *et al.* Establishment of a standard 14-3-3 protein assay of cerebrospinal fluid as a diagnostic tool for Creutzfeldt–Jakob disease. *Lab Invest* 2010;90:1637–44.
12. Kitamoto T, Shin RW, Doh-ura K, *et al.* Abnormal isoform of prion proteins accumulates in the synaptic structures of the central nervous system in patients with Creutzfeldt–Jakob disease. *Am J Pathol* 1992;140:1285–94.
13. Kitamoto T, Ohata M, Doh-ura K, *et al.* Novel missense variants of prion protein in Creutzfeldt–Jakob disease or Gerstmann-Sträussler syndrome. *Biochem Biophys Res Commun* 1993;191:709–14.
14. Shimizu S, Hoshi K, Muramoto T, *et al.* Creutzfeldt–Jakob disease with florid-type plaques after cadaveric dura mater grafting. *Arch Neurol* 1999;56:357–62.
15. Satoh K, Shirabe S, Eguchi H, *et al.* 14-3-3 protein, total tau and phosphorylated tau in cerebrospinal fluid of patients with Creutzfeldt–Jakob disease and neurodegenerative disease in Japan. *Cell Mol Neurobiol* 2006;26:45–52.
16. Atarashi R, Satoh K, Sano K, *et al.* Ultrasensitive human prion detection in cerebrospinal fluid by real-time quaking-induced conversion. *Nat Med* 2011;17:175–8.
17. Hirai T, Korogi Y, Arimura H, *et al.* Intracranial aneurysms at MR angiography: effect of computer-aided diagnosis on radiologists' detection performance. *Radiology* 2005;237:605–10.
18. Kallenberg K, Schulz-Schaeffer WJ, Jastrow U, *et al.* Creutzfeldt–Jakob disease: comparative analysis of MR imaging sequences. *AJNR Am J Neuroradiol* 2006;27:1459–62.
19. Murata T, Shiga Y, Higano S, *et al.* Conspicuity and evolution of lesions in Creutzfeldt–Jakob disease at diffusion-weighted imaging. *AJNR Am J Neuroradiol* 2002;23:1164–72.
20. Parchi P, Giese A, Capellari S, *et al.* Classification of sporadic Creutzfeldt–Jakob disease based on molecular and phenotypic analysis of 300 subjects. *Ann Neurol* 1999;46:224–33.
21. Meissner B, Kallenberg K, Sanchez-Juan P, *et al.* MRI lesion profiles in sporadic Creutzfeldt–Jakob disease. *Neurology* 2009;72:1994–2001.
22. Diagnostic criteria for sporadic CJD from 1 January 2010. *National Creutzfeldt–Jakob Disease Surveillance Diagnostic Criteria [online].* http://www.cjd.ed.ac.uk/criteria.htm (accessed 3 Oct 2011).
23. Young GS, Geschwind MD, Fischbein NJ, *et al.* Diffusion-weighted and fluid-attenuated inversion recovery imaging in Creutzfeldt–Jakob disease: high sensitivity and specificity for diagnosis. *AJNR Am J Neuroradiol* 2005;26:1551–62.
24. Lin YR, Young GS, Chen NK, *et al.* Creutzfeldt–Jakob disease involvement of rolandic cortex: a quantitative apparent diffusion coefficient evaluation. *AJNR Am J Neuroradiol* 2006;27:1755–9.
25. Fujita K, Nakane S, Harada M, *et al.* Diffusion tensor imaging in patients with Creutzfeldt–Jakob disease. *J Neurol Neurosurg Psychiatry* 2008;79:1304–6.
26. Hamaguchi T, Kitamoto T, Sato T, *et al.* Clinical diagnosis of MM2-type sporadic Creutzfeldt–Jakob disease. *Neurology* 2005;64:643–8.

症例報告

長大な脊髄病変をともないmultiple biopsiesにて組織診断された血管内リンパ腫の1例

白井　慎一[1)*]　高橋　育子[1)4)]　加納　崇裕[1)]　佐藤　和則[1)4)]
久保田佳奈子[2)]　矢部　一郎[1)]　村山　繁雄[3)]　佐々木秀直[1)]

要旨：左下肢筋力低下と右大腿後面の感覚低下・異常感覚を発症した45歳男性例を報告する．MRIにて胸髄病変をみとめ，脊髄炎として2度のステロイドパルス療法を施行したが奏功せず，完全対麻痺となった．MRI所見も増悪し，脊髄病変の長大化をみとめた．その後も脊髄症の増悪をみとめ，脊髄，皮膚，直腸，骨髄，筋，腎臓の生検，脾摘を施行した．そのうち，腎生検検体からIVLの病理所見をえることができた．ステロイド治療が奏功しない長大な脊髄病変では，IVLにともなう脊髄症を鑑別診断の1つに加える必要がある．確定診断には神経放射線学的検査をふくめた全身検索と，その結果に基づいた徹底的な組織生検をおこなうことが重要である．

（臨床神経 2012;52:336-343）
Key words：血管内リンパ腫，脊髄症，ステロイド，脊髄生検，腎生検

はじめに

血管内リンパ腫（intravascular lymphoma，以下IVL）はリンパ腫細胞が血管内に限局して増殖するnon-Hodgkin lymphomaの亜型であり，2008年のWHO分類ではintravascular large B-cell lymphomaと呼称されている[1]．血管外への浸潤が少なく，リンパ節の腫大ともなわない．腫瘍細胞による小血管の閉塞と，それにともなう血管壁の肥厚，内腔の狭窄，血栓の形成などの変化により全身の臓器に虚血病変をおこしえるが，とくに脳・脊髄・神経根に虚血性病変をおこすことが多く，急性発症の神経症候で初発することが多い[2]．今回われわれは，脊髄生検では電子顕微鏡検索で脱髄軸索をみとめたが原因を特定できず，腎生検でのみ診断することができたIVL症例を経験した．本症例は3椎体以上の長大な脊髄病変をきたし，ステロイド治療が無効であった．IVLにともなう脊髄病変を診断する上で貴重な症例と考えられたため，ここに報告する．

症　例

症例：45歳　男性
主訴：両下肢筋力低下
既往歴：42歳時　左肩脱臼．
家族歴：姉　関節リウマチ．
現病歴：2009年6月，左下肢筋力低下と右大腿後面の感覚低下・異常感覚をみとめた．異常感覚は端座位で増強され，臥位で消失していた．同年10月には左下肢筋力低下が進行し，跛行となったが，1カ月後には筋力低下は自然軽快し，右大腿の感覚低下のみが残存した．2010年1月に排尿困難感が出現し，近医泌尿器科受診したが前立腺疾患をふくめ，泌尿器科的異常を指摘されなかった．ついで近医整形外科を受診したが，整形外科的異常も指摘されなかった．2010年6月，近医神経内科初診し，右大腿後面の感覚低下，異常感覚，右アキレス腱反射低下をみとめ，胸椎MRIにてTh10～11椎体レベルに灰白質中心に両側の後索・側索を一部ふくむ全周性のT_2強調画像異常高信号をみとめ，同部位は増強効果をともなっていた（Fig. 1a, b）．脱髄，感染，膠原病，血管障害などを念頭に入院精査をおこなったが確定診断にはいたらず，両下肢筋力低下が出現したため，同院入院第14病日からステロイドパルス療法（メチルプレドニゾロン1g/日3日間）を施行し，その後療法としてプレドニゾロン（PSL）経口投与を60mgから開始し，3日ごとに10mg漸減した．しかしながら，排尿障害は進行し，ほぼ尿閉状態になった．胸椎造影MRIでは増強効果が消失するも，病変サイズには著変がなかったため，横断症状への進行と考え，同院入院第23病日から再度ステロイドパル

*Corresponding author: 北海道大学大学院医学研究科神経病態学講座神経内科学分野〔〒060-8638　札幌市北区北15条西7丁目〕
1)北海道大学医学研究科神経内科学
2)北海道大学病院病理部
4)東京都健康長寿医療センター
現　JA北海道厚生連帯広厚生病院神経内科
（受付日：2011年6月10日）

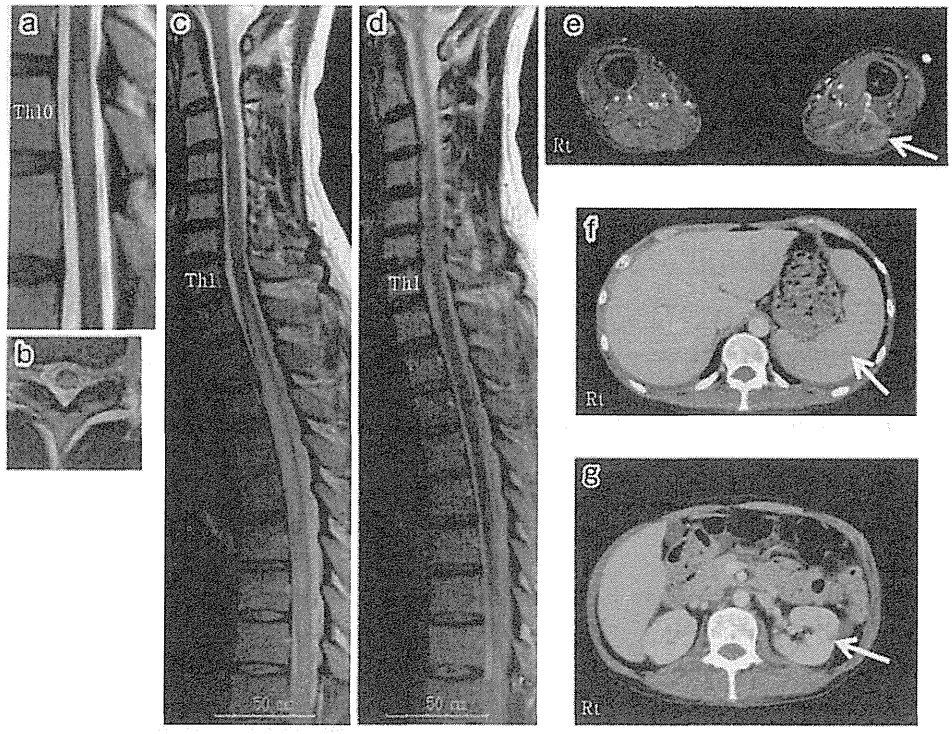

Fig. 1　Magnetic resonance imaging (MRI) of the spine (1.5T T_2 weighted image: TR 2,500 ms; TE 120 ms) and femoral muscles (1.5T short T_1 inversion recovery image, TR 3,900 ms, TE 76 ms) and abdominal computed tomography (CT).
(a) Sagittal MRI. Th 10-level axial MRI (b) at 2 months before admission to our hospital, (c) on the 53rd hospital day, before he was treated with R-CHOP therapy, and (d) on the 99th hospital day, when the 2nd round of R-CHOP therapy was performed and a T_2 weighted image showing a reduction in the high-intensity area. (e) MRI of the femoral muscles showing a high-intensity area in the left biceps femoris (arrow).
Abdominal CT on the 23rd hospital day showing (f) splenomegaly (arrow) and (g) left renal lesion (arrow).

スを施行した．しかし，その後も尿閉には変化なく，両下肢の脱力は進行し，再ステロイドパルス療法8日後には自力歩行困難となり，10日後には立位保持不可能となった．この時点で脊髄腫瘍の可能性もふくめ更なる検査を予定していたが，患者・家族から希望があり，前医神経内科に転院した．転院後も症状は進行し，ベタメサゾン4mg/day静注と高圧酸素療法を施行されたが，効果はみられなかった．同院で脊髄生検が施行された．ピースミールに採取された1mm大の標本4個について，ホルマリン固定パラフィン包埋光顕観察標本2個，エポン包埋電顕観察用標本2個を作製した．光顕ではHE染色でマクロファージの浸潤を，髄鞘染色（Klüver-Barrera染色）と軸索染色（Bodian染色）で，後者で保たれ前者で染色性の低下した部位をみとめ，脱髄の所見が示唆された．電顕観察では，髄鞘を持たない軸索をみとめた．またマクロファージ内にミエリン構造をみとめた．以上の光顕・電顕所見より，脱髄と診断した（Fig. 2）．更なる精査目的に2010年8月当院転院した．

入院時所見：身長172cm．体重51kg．脈拍68/min．血圧110/68mmHg，体温37.2℃．

眼瞼結膜に貧血無く，表在リンパ節は触知しなかった．肝脾は触れず，明らかな皮疹もみとめなかった．神経学的には脳神経系には異常なく，小脳性運動失調をみとめなかった．弛緩性対麻痺（近位・遠位筋ともに徒手筋力テスト0～1レベル）をみとめ，膝蓋腱反射は両側対称性に亢進し，アキレス腱反射も左優位に両側亢進し，Babinski反射，Chaddock反射はともに両側陽性であった．加えて，境界明瞭なTh10レベル以下の触覚・温痛覚・振動覚低下があり，感覚過敏帯はみとめなかった．同レベル以下の明らかな発汗低下や自動運動はみとめられず，腹壁反射・腹直筋反射は亢進し，Beevor徴候は陽性であった．尿閉のため尿道カテーテル留置されており，便失禁の状態であった．座位保持は困難であった．横断性脊髄障害の所見と考えられた．

検査所見：血算ではWBC 10,300/μl（白血球分画正常），RBC 374万/μl，Hb 12.6g/dl，Plt 16.2万/μlと軽度のWBC上昇をみとめた．生化学ではAlb 3.3g/dl，LDH 283U/lと軽度の低アルブミン血症とLDHの境界高値をみとめた．CRPは

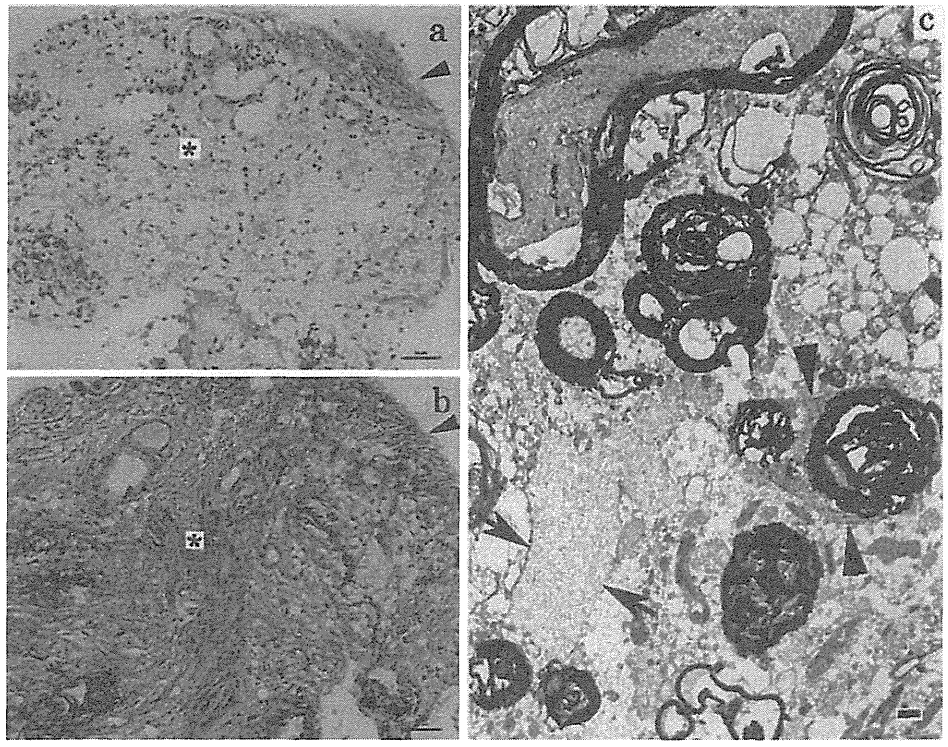

Fig. 2　Neuropathology of the spinal cord biopsy specimens at the Th10 level.
a) Relatively preserved myelinated axons (arrowhead) adjacent to an area with loss of myelination (asterisk). (Klüver-Barrera stain, bar = 50 μm)
b) Well-preserved axons in both the area of myelination (arrowhead) and the area of demyelination (asterisk) seen in section a. (Bodian stain, bar = 50 μm)
c) Ultramicrograph of the area of demyelination (double stained with uranyl acetate and lead citrate, bar = 1 μm) showing a demyelinated axon (arrows) and myelinophagia (arrowheads).

基準値内であったが赤沈は1時間値で51mmと軽度の亢進をみとめた．IgA，IgMは基準値内であったが，IgGは783 mg/dlと低下しており，2回のステロイドパルス療法による影響と考えられた．免疫学的には可溶性IL2レセプターが2,666U/ml（基準値0～459U/ml）と上昇をみとめ，抗核抗体40倍（核小体型），SS-A抗体14.0 indexをみとめた．IgEが694.1IU/mlと高値であったが抗寄生虫抗体スクリーニングは陰性であった．抗アクアポリン4抗体は陰性であった．血中HHV-6 DNA PCR，EBV-DNA PCR，サイトメガロウイルス抗原血症検査，トキソプラズマ抗体，クオンティフェロンはいずれも陰性であった．

髄液検査では，初圧170mm H_2O，終圧50mm H_2O，細胞数2/μl，蛋白92mg/dl，Cl 118mEq/l，糖78mg/dl，髄液可溶性IL2レセプター検出感度以下，髄液ACE 1.5U/l，IgG index 0.58，ミエリン塩基性蛋白459pg/ml，オリゴクローナルバンド陰性，HSV-DNA PCR陰性であった．髄液各種ウイルス抗体価は既感染パターンで血清抗体価との比も検討したが有意な上昇はみとめず，トキソプラズマ抗体も陰性であった．

画像所見：脊髄MRIではTh8/9～Th11/12椎体レベルの脊髄内，中心優位だがほぼ横断性にT_2強調画像高信号をみとめ腫大し，造影MRIではTh10～11椎体レベルの脊髄病変の中心部に軽度増強像をみとめたが，頸髄，腰髄のいずれにおいても神経根には腫大も造影効果もみとめなかった．脳MRIでは特記すべき所見をみとめなかった．CT-angiographyを施行したが，脊柱管内に拡張した血管構造はみとめず，AVMはみとめられなかった．FDG-PETでは，Th9～12椎体レベルの脊髄病変をふくめ異常集積をみとめなかった．胸腹部造影CTでは脾腫をみとめるのみで，その他明らかな異常をみとめなかった．

入院後経過（Fig. 3）：入院後から午後を中心に38℃台の発熱があり，10kg近い体重減少もみとめることから，腫瘍，とくにIVLによる病態をうたがい，random skin biopsy[3]，骨髄生検を施行したが，いずれも腫瘍細胞の特定にいたらなかった．また，上部消化管内視鏡検査では病的所見をみとめなかったが，大腸内視鏡検査施行時に直腸に発赤をみとめたので，同部位から生検を施行したが，異型細胞はみとめなかった．髄液細胞診を3度施行し，そのうち1回にのみ異型細胞をみとめたが，細胞数はごく少数のみであり，class分類不可能であった．

入院後MRIでTh4椎体レベルにまで脊髄異常信号が拡大

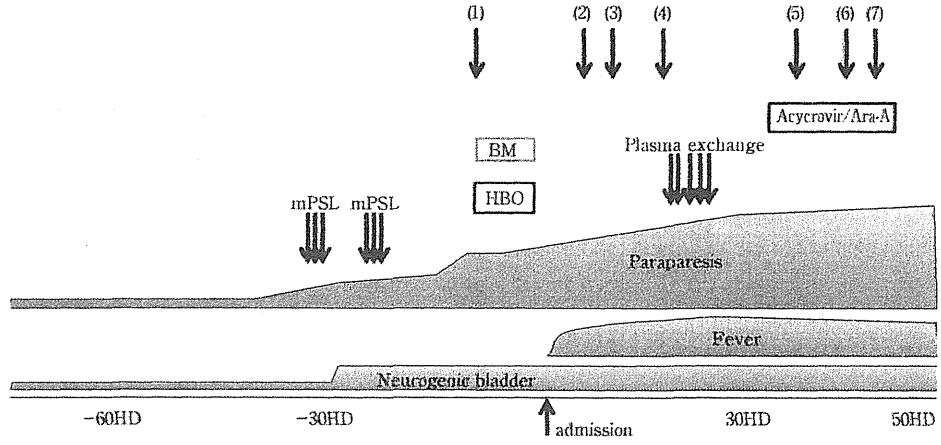

Serum sIL2R (U/ml)		2,666	1,201	
CSF				
cell (/μl)		2	16	8
protein (mg/dl)		92	200	257
atypical cell		(−) (−)	(+)	

Fig. 3 Clinical course.
Paraparesis exacerbated during the course of methylprednisolone pulse therapies, hyperbaric oxygen therapy, plasma exchanges, and intravenous acyclovir and Ara-A. (1) Spinal cord biopsy performed at another hospital. For making a definite diagnosis, we performed (2) a random skin biopsy, (3) rectal biopsy by using a colon fiberscope, (4) bone marrow biopsy, (5) muscle biopsy, (6) CT-guided renal biopsy, and (7) a splenectomy. HD: hospital days; BM: betamethasone.

したため，免疫介在性の病態を考慮して，第17病日から第26病日まで血漿交換を5回施行したが，血漿交換終了後にはTh2椎体レベルにまで異常信号が更に拡大した．また，第32病日から46病日まで，ウイルス性脊髄炎の可能性も考え，アシクロビルとビタラビンを併用した．治療と並行して精査を継続し，第12病日の筋MRIでは左大腿二頭筋にSTIR高信号（Fig. 1e）を，第23病日の胸腹部造影CT再検では，脾腫の増大（Fig. 1f）と両側腎実質に前医入院時にはみとめなかった複数の造影不良病変をみとめた（Fig. 1g）．

臨床検査で腎機能異常はなく，尿細胞診も4回おこなったがいずれも陰性であった．これらの臨床経過と検査結果からIVLを強くうたがい，患者・家族から同意をえて，左大腿二頭筋長頭より筋生検を，左腎からCTガイド下に腎生検を，そして脾摘を施行した．大腿二頭筋生検が，IVLを念頭においた異型細胞検出を目的に施行されたが，異型細胞の検出にはいたらなかった．通常の光顕観察では，筋線維の大小不同があり炎症細胞浸潤はみとめなかった．小角化線維が散見されtype 2線維の萎縮がみとめられた．この結果は，廃用性変化に加えて神経原性変化を示唆する所見と考えられた．脾臓においても，赤脾髄の開大・鬱血と白脾髄の萎縮をみとめるのみであり，免疫染色もふくめて，IVLをうたがう所見はえられなかった．腎生検検体において，間質の血管内に不整形の核を有するCD20陽性，CD3陰性の大型異型細胞が充満し，intravascular large B-cell lymphomaの所見がみとめられた（Fig. 4）．リンパ腫細胞の血管内浸潤部位では尿細管脱落所見をみとめていたが，糸球体には有意な所見はみとめなかった．

以上よりIVLにともなう脊髄症と診断し，化学療法目的に第58病日に血液内科転科となった．転科時には脊髄MRIでのT_2強調画像高信号領域はTh2椎体レベルまで拡大していたが（Fig. 1c），転科後R-CHOP療法を施行し，2コース終了後の脊髄MRIでT_2強調画像高信号領域は著明に縮小し（Fig. 1d），6コース終了時点で寛解と判断した．発症から2年2カ月経過した現時点で再発所見をみとめず，血清可用性IL2レセプターも316U/mlと正常化しているが，Th7レベル以下の弛緩性対麻痺があり歩行不能である．

考　察

IVLは神経学的異常・皮膚病変を主徴とし，高齢者に後発するびまん性大細胞型B細胞リンパ腫のまれな亜型として位置づけられており，2008年発行のWHO分類では中小血管内における腫瘍性B細胞の浸潤という病理像により定義される，成熟型B細胞リンパ系腫瘍の一疾患単位として取り扱われている[1]．生前診断は難しく，剖検で確定診断される例がほとんどであったが，近年では疾患自体の認識が高まったことと検査技術の進歩により，生前診断される例が散見される[2]．さらに，CD20モノクローナル抗体rituximabをもちいた化学療法の有効性も報告されている[4]．

今回提示した症例は，下肢感覚異常，排尿障害で発症し，胸腰髄に長大な病変をきたした症例である．ステロイドパルス

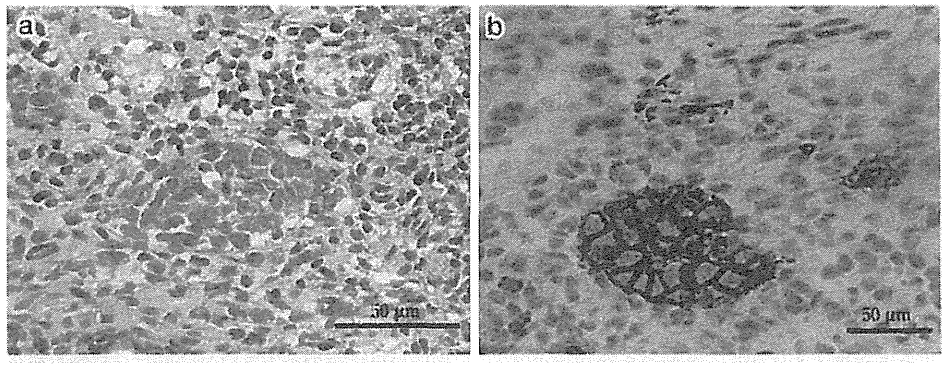

Fig. 4 Pathological examination of the left renal lesion.
Large lymphoid cells were congested in the vessels of the renal stroma (a: hematoxylin and eosin [HE] staining, bar＝50 μm); these cells were positive for CD20 (b: anti-CD20 staining, bar＝50 μm) and negative for CD3.
These findings are compatible with intravascular large B-cell lymphoma.

Table 1 Reported cases of spinal intravascular lymphoma.

Patients	Symptoms	The level of the spinal lesion	Lesions	Diagnosis	Steroid response	Author
60s M	Dysesthesia in the legs	ND	ND	Autopsy	ND	Saito, et al[5]
60s M	Dysesthesia in the legs	ND	ND	Muscle biopsy	ND	Nakahara, et al[6]
40s M	Conus medullaris syndrome	Conus medullaris	3 vertebral bodies	Autopsy	+	Schwarz, et al[7]
70s F	FUO, TIA-like symptoms, retinopathy	Lumbar cord	Multiple patchy lesions	Bone marrow biopsy, PET	ND	Hoshino, et al[8]
70s M	Paraplegia, Korsakoff-like symptoms	Cervical and thoracic cord	Multiple patchy lesions	Cytology of CSF	ND	Baehring, et al[9]
70s M	Tetraplegia	Thoracic and lumbosacral cord	Enlarged and enhanced lesion	Clonal IgH gene rearrangement in CSF	ND	Baehring, et al[9]
30M	Headache, abnormal behavior, paraplegia, urinary incontinence	Th 2 level	2 vertebral bodies	Liver biopsy	+	Abe, et al[10]
50s M	Paraplegia, urinary incontinence	Lower thoracic-lumbar cord	More than 9 vertebral bodies	Nasal polyp and muscle biopsy	ND	Takizawa, et al[11]
70s M	Progressive paraplegia, sensory loss of legs.	ND	ND	Autopsy	ND	Yang T, et al[12]
40s M	Dysesthesia in legs, urinary incontinence	ND	ND	Bone marrow biopsy	ND	Savard, et al[13]
40s F	Conus medullaris syndrome	(−)	ND	Bone marrow biopsy	ND	Tsugawa, et al[14]
80s F	Lower limb weakness and numbness.	Th 10 level	7 vertebral bodies	Autopsy	ND	Kumar, et al[15]
40s M	Dysesthesia in the legs → paraplegia	Th 12 level	17 vertebral bodies longitudinal lesion	Renal biopsy	−	Our case

ND: Not documented;
FUO: Fever of unknown origin;
+ : Effective;
− : Ineffective.

療法が奏効しなかったことから，自己免疫介在性の病態の他に，腫瘍，血管障害，感染などを鑑別するために全身精査をおこなった結果，IVLと診断することができたが，過去の報告同様，確定診断にいたるまで長期間を要した．過去の脊髄IVLの報告例をTable 1に示す[5)～15)]．これらの報告例においても，本症例と同様に下肢感覚異常，排尿障害などで発症している症例が多いが，本症例のように脊髄長大病変をきたした例は剖検で診断した1例のみである[15)]．化学療法後に脊髄MRI異常信号が改善したことを記載しているものはなく，本症例がはじめてである．脊髄梗塞の自然経過でも一過性の脊髄MRI異常信号となるが，2010年6月から化学療法開始まで脊髄異常信号が拡大する一方で化学療法開始後には異常信号が縮小しており，化学療法が信号改善に寄与していたと考えられた．電顕所見で脱髄所見があることから，本症例の脊髄病変はIVL腫瘍塞栓による微小循環不全・脊髄梗塞にともなう浮腫性変化である可能性に加えて，何らかの免疫機序にともなう病態が背景にある可能性も否定できない．

また，本症例の発病初期には，下肢異常感覚，筋力低下がみ